Inventory of Supplemental Information for Philip et al.

3 Supplemental tables

5 Supplemental figures with legends

Experimental Procedures

Supplemental References

Supplemental information

Coincidence Detection by Two-State Allosteric Enzymes:

Synergistic Activation of Phospholipase C-β3 by $G\alpha_q$ and $G\beta\gamma$

Finly Philip, Ganesh Kadamur, Rosa González Silos, Jimmy Woodson and Elliott M. Ross

3 Supplemental tables
5 Supplemental figures with legends
Experimental Procedures
Supplemental References

Fig. S1

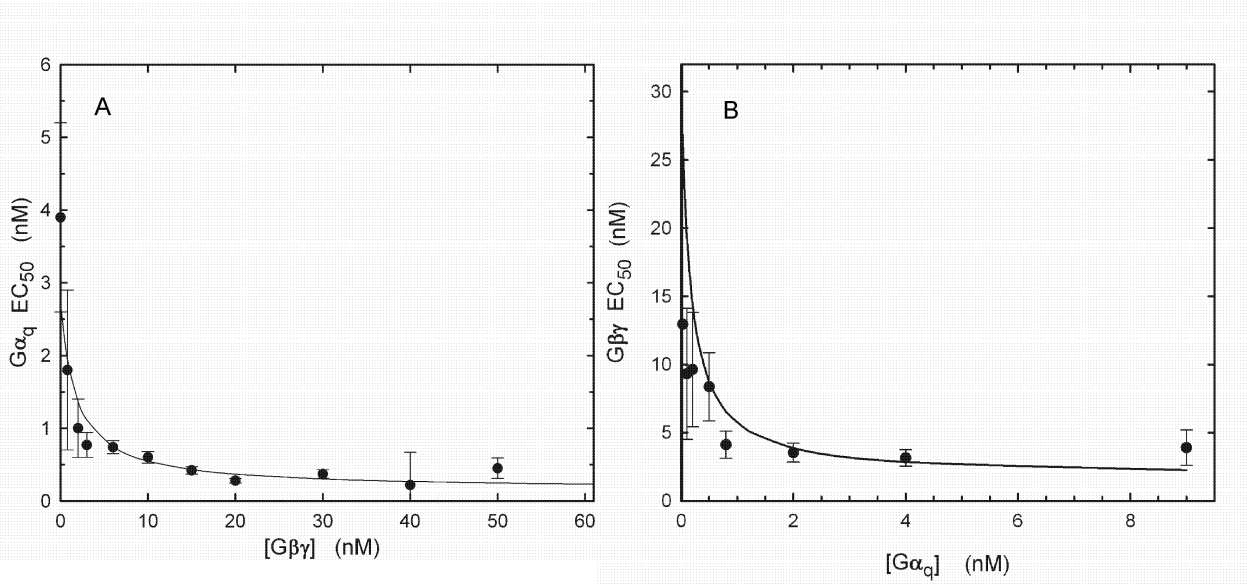

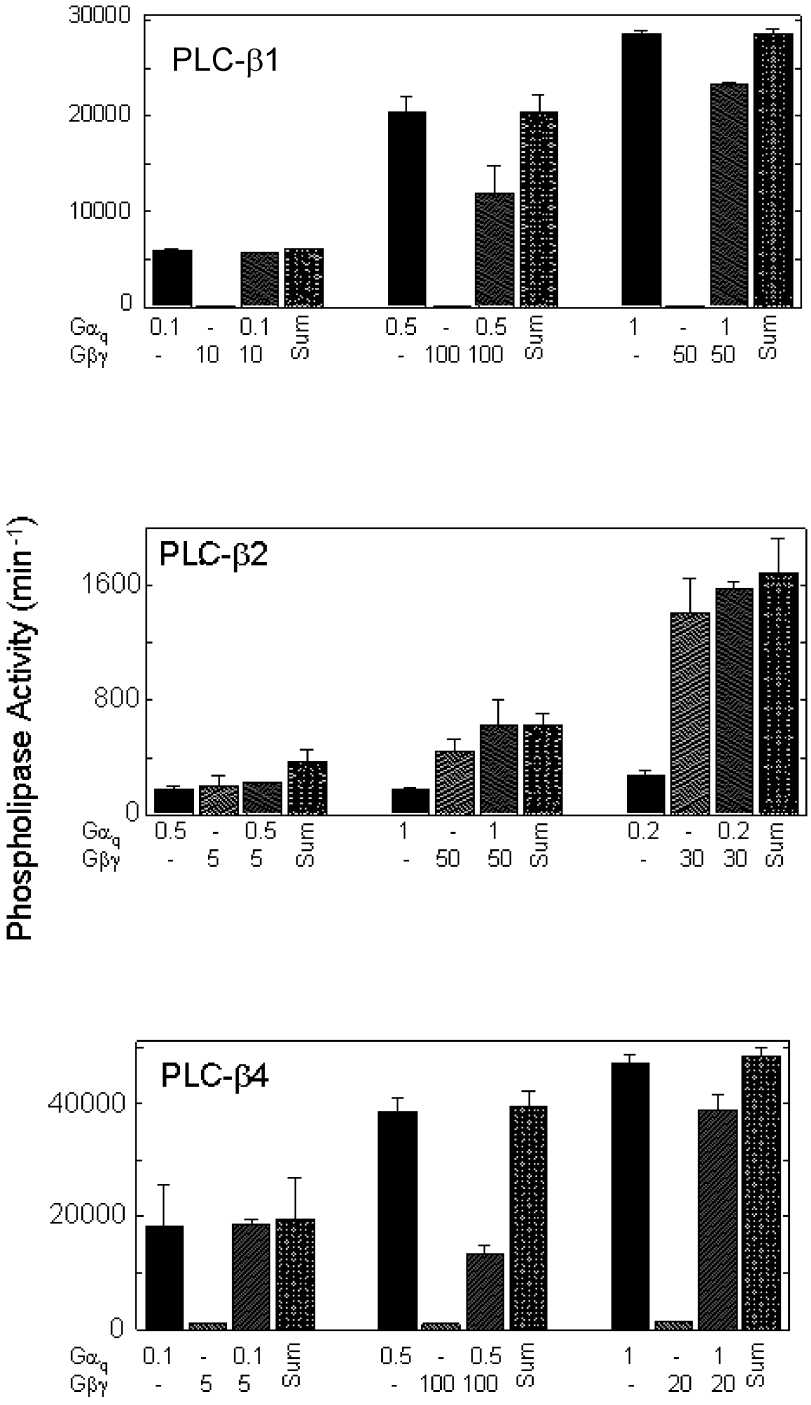
PLC-β1
PLC-β2
PLC-β4
Phospholipase Activity (min-1)
30000
20000
10000
0
1600
800
40000
Gαq
Gβγ
0.1 - 0.1 Sum
- 10 10
0.5 - 0.5 Sum
- 100 100
1 - 1 Sum
- 50 50
0.5 - 0.5 Sum
- 5 5
1 - 1 Sum
- 50 50
0.2 - 0.2 Sum
- 30 30
0.1 - 0.1 Sum
- 5 5
0.5 - 0.5 Sum
- 100 100
1 - 1 Sum
- 20 20

Figure S3

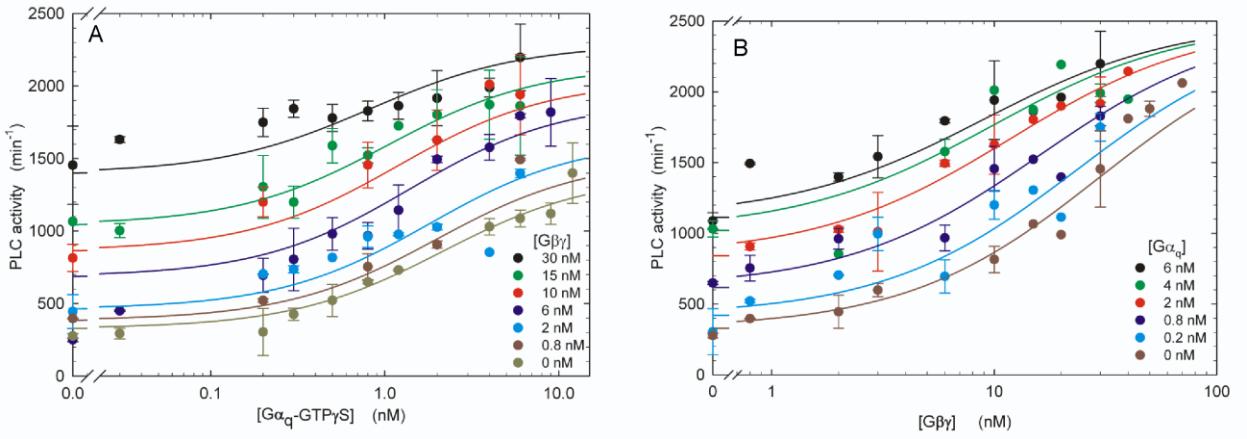
A
PLC activity (min^{-1})
2500
2000
1500
1000
500
0
0.0
0.1
1.0
10.0
[Gαq-GTPγS] (nM)
[Gβγ]
30 nM
15 nM
10 nM
6 nM
2 nM
0.8 nM
0 nM
B
PLC activity (min^{-1})
0
1
10
100
[Gβγ] (nM)
[Gαq]
6 nM
4 nM
2 nM
0.8 nM
0.2 nM
0 nM

Figure S4

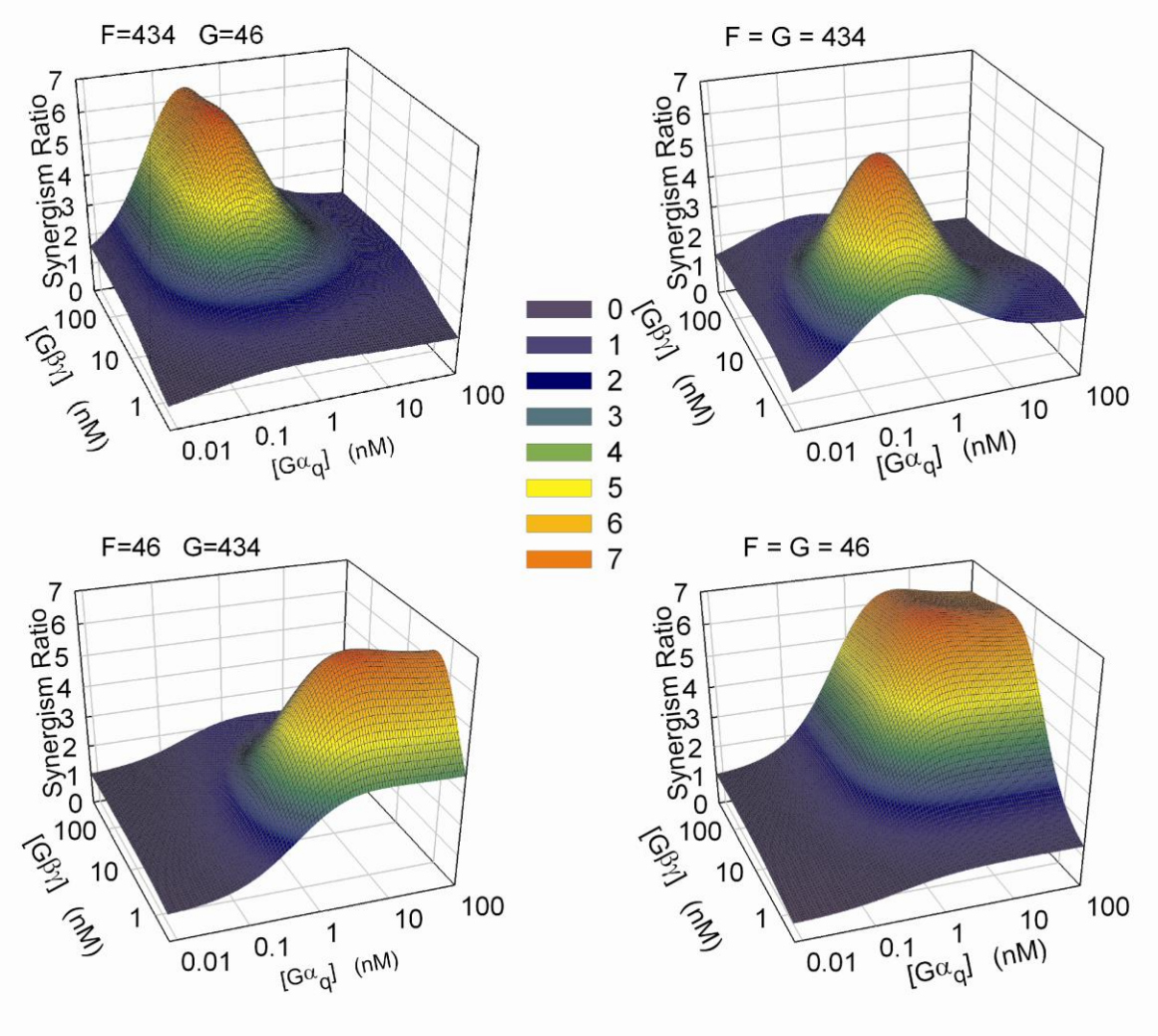
F=434 G=46
F = G = 434
F=46 G=434
F = G = 46
Synergism Ratio
0
1
2
3
4
5
6
7
[Gβγ] (nM)
100
10
1
0.01
0.1
1
10
100
[Gαq] (nM)

Figure S5

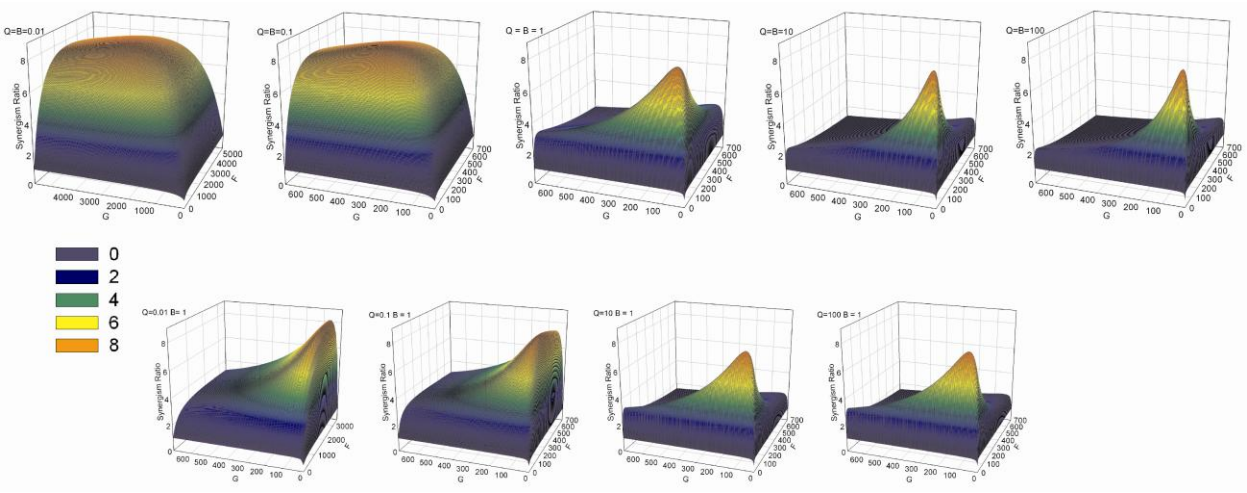
Q=B=0.01
Q=B=0.1
Q = B = 1
Q=B=10
Q=B=100
Synergism Ratio
G
K
0
2
4
6
8
Q=0.01 B= 1
Q=0.1 B = 1
Q=10 B = 1
Q=100 B = 1

Table SI. Multiple Gβγ isoforms synergize with $G\alpha_q$

$G\alpha_q$	Gβγ	PLC Activity (min^{-1} ± SD)	Synergism Ratio
+	---	547 ± 4	
-	+Gβ1γ2	24 ± 3	3.9
+	+Gβ1γ2	2250 ± 52	
-	+Gβ1γ3	74 ± 1	4.6
+	+Gβ1γ3	2840 ± 222	
-	+Gβ1γ5	110 ± 9	4.5
+	+Gβ1γ5	2970 ± 189	
-	+Gβ2γ5	66 ± 12	3.9
+	+Gβ2γ5	2370 ± 115	

PLC-β3 was assayed in the presence of four different Gβγ isoforms, 5 nM each, with and without 0.5 nM $G\alpha_q$. These Gβγ preparations were purified without the final anion exchange step and therefore produced lower activities because of excess detergent in the assays. Similar results, *i.e.* minimal difference in synergism ratios among the Gβγ preparations, were obtained in other experiments using other concentrations of $G\alpha_q$ and Gβγ.

Table SII. $G\alpha_q$ must be activated to synergize with $G\beta\gamma$.

Additions	PLC Activity (min^{-1})	Synergism ratio
None	36 ± 3	
20 nM $G\alpha_q$-GDP	45 ± 3	
20 nM $G\beta\gamma$	178 ± 29	
Both	242 ± 64	0.92
0.2 nM $G\alpha_q$-GTPγS	235 ± 8	
20 nM $G\beta\gamma$	178 ± 29	
Both	1630 ± 60	5.8
20 nM $G\alpha_q$-GDP	45 ± 3	
30 nM $G\beta\gamma$	238 ± 28	
Both	263 ± 16	0.93

PLC-β3 activity was measured in the presence of the G protein subunits shown. $G\alpha_q$ was bound either to GDP or GTPγS. Values are means, ± SD, of triplicate determinations except for $G\alpha_q$-GDP, where n=6. Activity for 20 nM $G\alpha_q$-GDP alone is listed twice for clarity in the table. Data are representative of results of 3 separate experiments.

Table SIII. Model parameters for PLC-β2 at 60 nM Ca^{2+}

	Matrix Fit
Z	2500 ± 130 min^{-1}
J	0.15 ± 0.015
K_q	0.240 ± 0.062 nM^{-1}
F	8.2 ± 1.4
K_b	0.00061 ± 0.00037 nM^{-1}
G	410 ± 120

Values for the parameters, ± SE, of the allosteric model (Figure3) were estimated by fitting data from the experiment shown in Figure S2, but with additional data not shown included to improve the quality of the fit. Z is the maximum activity of the PLC-β2 under these assay conditions, with units of mol PIP_2 hydrolyzed /min / (mol PLC).

Legends for supplemental figures

Figure S1. $G\alpha_q$ and $G\beta\gamma$ each decrease the EC_{50} value of the other for activation of PLC-β3. Data are from the experiment shown in Figure 3. The EC_{50} values are derived from mid-points (± 95% confidence limits) of individual concentration-activity curves for one G protein subunit at selected concentrations of the other. Fits were based on a single-site saturation equation. The solid lines are calculated using the parameters of Table II, and show that each G protein subunit decreases the EC_{50} of the other approximately 19-fold. This relative change is equal to the calculated change in the equilibrium binding constant for one subunit that is caused by a saturating amount of the other.

Figure S2. PLC-β1, PLC-β2 and PLC-β4 do not display $G\alpha_q$-$G\beta\gamma$ synergism. Activities of PLC-β1, PLC-β2 and PLC-β4 were assayed in the presence of $G\alpha_q$, $G\beta\gamma$ or both, each at the concentrations shown below the graphs. Three sets of data, ± SD, are shown for each PLC-β isoform, and the fourth bar in each set shows the sum of activities measured with $G\alpha_q$ or $G\beta\gamma$ alone. PLC-β1 and PLC-β4 were assayed at 1 μM Ca^{2+} and PLC-β2 was assayed at 60 nM Ca^{2+}. These results are representative of multiple experiments at diverse concentrations of PLC-β, Ca^{2+} and each G protein subunit. Unstimulated activities in these experiments were PLC-β1, 72 min^{-1}; PLC-β2, 69 min^{-1}; PLC-β3, 1210 min^{-1}. For reference, unstimulated activity for PLC-β3 in the experiment of Figure 1B was 7 min^{-1} at 60 nM Ca^{2+} and 89 min^{-1} at 1 μM Ca^{2+}.

Figure S3. Independent (non-synergistic) regulation of PLC-β2 by $G\alpha_q$ and $G\beta\gamma$. PLC-β2 activity was assayed at 60 nM Ca^{2+} over a range of concentrations of $G\alpha_q$ and $G\beta\gamma$ chosen to optimize fitting the data to the allosteric model of Figure 2. Activities are plotted against the concentration of $G\alpha_q$ (panel A) and $G\beta\gamma$ (panel B) at various fixed concentrations of the other subunit. The data sown in the graphs were selected from a set of 92 duplicate determinations. Solid lines are simulations based on the model and the parameter values obtained in the fit (Table SIII).

Figure S4. Dependence of synergism on the concentrations of G protein subunits at varying values of the bias constants F and G. To determine the interplay of G protein concentration and the bias constants F and G, the dependence of synergism ratios on concentration was simulated for four F,G pairs. Values of K_b, K_q and J = 0.0015 were from Table II. Maximal synergism is constant for all conditions, but the steepness of the peak and its symmetry vary according to values of F and G. The upper left panel uses F,G values from the fitting to the data of Figure 3. The right two use either the higher or lower value for both F and G, and the lower left panel has F and G reversed from the experimentally determined values. For equal values of F and G (top panels), synergism peaks symmetrically at an intermediate concentration of each subunit. At high values of F and G, the peak is sharp. At lower values, the peak becomes a broad plateau, such that significant synergism is displayed over a wide range of activator concentrations. For unequal values of F and G (left panels), synergism remains high along a ridge that extends to very high concentrations of the G protein subunit with the lower bias constant. The ridge falls off at high concentrations of the subunit with the higher bias constant. The general dependence of peak symmetry on F and G is independent of J, but peaks become lower and more sharp as J increases (Figure 5).

Figure S5. Synergism is more pronounced and less sensitively dependent on F and G when G protein concentrations are low. The synergism ratio for PLC-β3 was simulated for varied concentrations of $G\alpha_q$ and $G\beta\gamma$ with J=0.0015 (Table II). G protein concentrations are listed as reduced concentrations, the product of the actual concentration and the association equilibrium constant with reduced [$G\alpha_q$] abbreviated as Q and reduced [$G\beta\gamma$] abbreviated as B. The upper five panels, with the concentrations of $G\alpha_q$ and $G\beta\gamma$ equal, show how increasing the concentrations sharpens the peak and finally decreases the maximum synergism that can be attained. However, at very low G protein concentrations, higher values of F and or G are needed for synergism. Thus both axes are extended 8-fold in the upper left panel. When the concentration of one G protein subunit is, as shown in the lower left two panels, the peak becomes asymmetric. The effect is large; the G axis of the lower left panel is extended 5-fold.

Supplemental Experimental Procedures

Protein purification

N-terminally His_6-tagged PLC-β1 (rat), PLC-β2 (mouse) and PLC-β3 (mouse) were purified as described for PLC-β1 [43]. PLC-β4 (human) was purified similarly but with slight modifications. PLC-β4 was extracted from Sf9 membranes with 1 M NaCl in buffer A (20mM NaHepes (pH 7.5), 1mM $MgCl_2$, 5 mM 2-mercaptoethanol, 10 μg/mL leupeptin, 1 μg/ml aprotinin and 0.1 mM PMSF). Extracted protein was stirred with Ni-NTA resin (GE) for 2 h in the presence of 0.1% Lubrol and 5mM imidazole. The resin was washed sequentially with buffer A plus 1 M NaCl, 0.1 % Lubrol and 5 mM imidazole and with buffer A plus 100 mM NaCl and 5 mM imidazole until A_{280} reached baseline. PLC was eluted with buffer A plus 100 mM NaCl and 150 mM imidazole. The eluate was diluted in buffer B (20 mM NaMES pH 6.0, 20 % glycerol, 1 mM DTT and 0.1mM EDTA) and loaded onto a Mono-S column that was equilibrated with buffer B. After washing the column with 100 mM NaCl in buffer, PLC was eluted by a gradient of 100-500 mM NaCl in Buffer B.

$G\alpha_q$ was purified as described [43]. To decrease the detergent:protein ratio, purified $G\alpha_q$ was diluted 5-fold in buffer C (20mM NaHepes (pH7.5), 0.1 mM EDTA, 1 mM DTT, 10 μM GDP, 0.5 % CHAPS and 1 mM $MgCl_2$), adsorbed to Mono-Q and washed with buffer C to replace cholate with CHAPS. $G\alpha_q$ was eluted with 300mM NaCl in buffer C, diluted 10-fold in buffer C, adsorbed to a 0.1 ml column of Q-Sepharose and eluted with 300mM NaCl in buffer C. For the experiment shown in Table SII, the $G\alpha_q$-GDP was this preparation with no additional treatment.

Gβγ was purified as described by Kozasa and Gilman [46], and then concentrated and switched to a CHAPS-containing buffer as was done for $G\alpha_q$. Gβ1γ2 was used for all experiments except those shown in Table SI.

Protein concentrations were determined by amido black binding [47].

$G\alpha_q$ was activated before assay by incubation at 30 ^oC with 1mM GTPγS in 50 mM

NaHepes (pH 7.5), 100 mM NaCl, 4 mM $MgCl_2$, 1 mM DTT, 50 mM $(NH_4)_2SO_4$, 0.1 mg/ml BSA and 0.4 % CHAPS [44]. Incubation was extended to 5 h such that any $G\alpha_q$ that had not bound GTPγS would be denatured [44] and would be unable to chelate Gβγ in the PLC assay. $G\alpha_q$ was activated at the highest concentration possible to minimize detergent in the PLC assay. The fraction of $G\alpha_q$ bound to GTPγS was determined by monitoring bound [^{35}S]GTPγS.

PLC assay, data analysis and fitting

PLC activity was measured by monitoring hydrolysis of [^{3}H]PIP_2 on the surface of large unilamellar vesicles (PE:PS:PIP_2, 20:4:1 molar ratio; 0.25 mM total phospholipid) [43,48]. Vesicles were prepared in 50 mM NaHepes (pH 7.5), 100 mM NaCl and 2 mM EGTA. PLC activity is proportional to the concentration of PIP_2 under these conditions. The assay times (2 - 40 min) and the concentration of PLC (10 - 4000 pM) were adjusted such that PIP_2 hydrolysis remained linear with time and PLC concentration. The concentration of PLC was also kept low enough that it did not substantially deplete the total concentration of activated $G\alpha_q$ in the assay. Assays were initiated by the addition of PLC at 37 ^{o}C. The final concentration of free Ca^{2+} in the assays was adjusted with an EGTA buffer that contained 2 mM EGTA and a concentration of $CaCl_2$ calculated according to the program Bound and Determined [45]. Data are expressed as moles of IP_3 produced per min per mole PLC.

The specific activities for PLC-βs under these assay conditions are relatively high, 45,000-60,000 min^{-1} at optimal [Ca^{2+}], [$G\alpha_q$] and [Gβγ] (Figure 1B). Because the PIP_2 substrate is 4 mol % of total lipids and activity increases linearly with substrate concentration in this range, higher activities would be observed with the higher PIP_2 concentrations that are frequently used. Cholate and CHAPS both inhibit PLC activity, with IC_{50}'s of 0.2 mM and 0.1 mM respectively under these conditions. The CHAPS concentration in the assays, derived from added G protein subunits, did not exceed 0.02 mM and was maintained equal among all samples within an assay.

Protein concentrations are reported in terms of the aqueous assay volume. However,

PLC-β, $G\alpha_q$ and Gβγ all bind to the surface of the substrate vesicles and occupy an annular shell volume about 5000-fold smaller. In addition, rotational mobility of the proteins is limited to one dimension. Values of K_b and K_q can be readjusted by factor to approximate actual protein-protein binding affinities, although the loss of two dimensions of rotational freedom mortgages thermodynamic comparisons with soluble reactions.

Assay data were fit using the Marquardt-Levenberg algorithm in either StatGraphic or SigmaPlot. Values for the parameters of the allosteric model (Figure 2) that are shown in Table II as "Matrix Fit" were derived by fitting a single data set for a PLC assay in which concentrations of $G\alpha_q$ and Gβγ were varied as shown in Figure 3. These data are representative of two other similar experiments. We were unable to fit data from all these experiments simultaneously because absolute activities vary among preparations of substrate vesicles. EC_{50} values for the G protein subunits vary 2- to 3-fold among experiments, presumably because of variable binding to the vesicles. Parameters for PLC-β2 shown in Table SIII were calculated similarly to those for PLC-β3.

Parameters for PLC-β3 shown as "4-point fits" (Table II) were derived from three separate experiments in which PLC activity (v in the equations below) was assayed in the presence of saturating concentrations of $G\alpha_q$, Gβγ (3 determinations in each experiment), both (6-8 determinations) or neither (4 determinations). Parameters were then calculated as Z = v for the combination of $G\alpha_q$ and Gβγ; J = v / Z without G protein; F = v/(J•(Z-v)) for $G\alpha_q$ alone; and G = v/(J•(Z-v)) for Gβγ alone. Data shown are the means of the values calculated from each experiment.

Supplemental References

46. Kozasa T. and Gilman A.G. (1995). Purification of recombinant G proteins from Sf9 cells by hexahistidine tagging of associated subunits. Characterization of α_{12} and inhibition of adenylyl cyclase by α_z**.** J. Biol. Chem. *270***:** 1734-1741.

47. Schaffner W. and Weissmann C. (1973). A rapid, sensitive, and specific method for the determination of protein in dilute solution**.** Anal. Biochem. *56***:** 502-514.

48. Blank J.L., Ross A.H., and Exton J.H. (1991). Purification and characterization of two G-proteins that activate the β1 isozyme of phosphoinositide-specific phospholipase C**.** J. Biol. Chem. *266***:** 18206-18216.